Effects of Optical and Geometrical Properties on YORP Effect for Inactive Satellites

Antonella A. Albuja and Daniel J. Scheeres
University of Colorado - Boulder , Boulder, CO, USA

ABSTRACT

The exponential growth of the amount of space debris found in Earth orbit has made it crucial to understand the dynamics and long term behavior of these objects. A number of observations of inactive satellites in geosynchronous Earth orbit (GEO) demonstrate that the rotational periods of these objects are evolving over time. Furthermore, this evolution can vary from satellite to satellite. The Yarkovsky-O'Keefe-Radzievskii-Paddak (YORP) effect has been shown to be the cause of the changing rotational dynamics of asteroids and has recently been introduced as a possible explanation for the observed changes in rotational period of inactive satellites in GEO. This effect however, is very dependent on optical, thermal and geometrical parameters of a satellite. This paper studies the sensitivity of the torques created by the YORP effect to changes in these parameters. This sensitivity analysis is used to determine possible long term behaviors for inactive satellites.

1. INTRODUCTION

Observations of inactive satellites in geosynchronous Earth orbit (GEO) have shown that the rotational periods of these satellites are changing over time [1]. In addition, the evolution of the rotational period of these satellites varied greatly from one satellite to the next. One satellite's rotational period might only increase while another's will only decrease and a third satellite's rotational period might experience a combination [1]. Observations of different types of GEO satellites have demonstrated that there is a wide range of rotational periods for these satellites. For satellites that were once spin stabilized the periods range from 2-7 seconds, for launch vehicles the periods range between 5-15 seconds and for 3-axis stabilized satellites the periods are between 15 - 500 seconds [1, 2]. With the growing number of space debris and need to find methods of removing inactive objects in orbit, it is very important to understand the evolving dynamics of these objects. In particular, it is crucial to understand potential long term behaviors for debris.

The Yarkovsky-O'Keefe-Radzievskii-Paddak (YORP) effect has been well studied and credited for the secular change in angular velocity and obliquity of asteroids [3, 4]. As photons are re-emitted as energy from the surface of an asteroid, a net forced acting opposite the normal of the surface is created [4]. In addition, a force is created from reflected sunlight from the surface of the asteroid [5]. These forces, which will not act directly through the center of mass (CM) of the asteroid, will create a net torque. While this torque is rather small, over large time periods it has been shown to cause a change in the asteroid's angular velocity and obliquity. Although this effect has been well documented for asteroids it has only recently been considered to be the cause of secular changes in the rotational period of inactive satellites [6]. Those results showed that the YORP effect could be the main cause of observed changes in rotational periods of inactive satellites.

Since the YORP effect results from light and thermal energy being reflected and re-emitted from the surface of a body, the moments that are created are highly dependent on optical and thermal properties of the body. Hence, the dynamical evolution of the angular velocity and obliquity of a satellite as a result of the YORP effect will be directly affected by optical and thermal properties of the satellite. The purpose of this paper is to explore the sensitivity of YORP torques to optical, thermal, and geometrical properties of an inactive satellite. This work uses the simplest satellite model to analyze how the YORP torques change as the optical, thermal and geometrical parameters are varied to account for all possible values. By analyzing the YORP torques and how they change with the various optical parameters possible long term behaviors for a satellite can be defined. First, a brief description of the YORP theory is given, followed by simplifications that can be made by using a simple satellite model. Next, the equations of motion for angular velocity and obliquity under YORP torques are defined. Then the satellite model used for this analysis is described and the Fourier coefficients used to describe the YORP moments are computed for various optical and thermal parameters. Lastly, possible long term behaviors based on the results are described.

2. ROTATIONAL DYNAMICS DUE TO YORP

This section gives a brief description of the moments that are created as a result of the YORP effect and provides some simplifications that can be made when using a simple satellite model. Next the equations of motion for the angular velocity and obliquity of a satellite under YORP moments is given. The theory presented here follows that described in reference 5. As such the following assumptions are made. First, the theory given assumes the body being analyzed is in a heliocentric orbit. This is accepted as we are focused on the long term behavior and therefore we focus only on the motion of the Earth about the Sun throughout a year which will cause any Earth orbiting satellite to trace an orbit around the Sun. In addition, we assume that the satellite is uniformly rotating about the z-axis in a body-fixed frame whose origin is located at the center of mass (CM) of the satellite and whose axes lie along the principle moments of inertia of the satellite, where the z-axis is the maximum moment of inertia. Lastly, we assume that the satellite being analyzed is broken up into multiple facets.

2.1. YORP Moments

As described in reference 5 the total moment acting on a satellite created by the YORP effect is a sum of the moments acting on each facet making up the surface of the satellite. This total moment can be expressed as a Fourier series as shown in Eq. 1, where λ_s is the longitude of the Sun in the body-fixed frame.

$$\frac{\vec{M}}{P(R)} = \vec{C}_0 + \sum_{n=1}^{\infty}[\vec{C}_n \cos(n\lambda_s) + \vec{D}_n \sin(n\lambda_s)] \tag{1}$$

The YORP coefficients ($\vec{C}_n$ and $\vec{D}_n$) can then be averaged over an orbital period around the Sun, these will be denoted by a bar above the coefficient. As defined in reference 5 only the $\bar{\vec{C}}_0$, $\bar{\vec{C}}_1$ and $\bar{\vec{D}}_1$ coefficients will affect the evolution of the angular velocity and obliquity. Therefore, we will only focus on those coefficients which are defined in Eqs. 2, 3 and 4, where $\vec{r}_i$ points from the CM to the center of the i^{th}facet, A_i is the area of the i^{th}facet, $\hat{n}$ is the vector normal to the i^{th}facet, ρ_i is the albdeo, s_i is how much of the reflected light is specularly reflected, $a_{2,i} = B(1-s_i)\rho_i + (1-\rho_i)B\left(\frac{\epsilon_{f,i}-\epsilon_{b,i}}{\epsilon_{f,i}-\epsilon_{b,i}}\right)$, B is the Lambertian scattering coefficient, $\epsilon_{f,i}$ is the emissivity of the front of a facet and $\epsilon_{b,i}$ is the emissivity of the back.

$$\bar{\vec{C}}_0 = \sum_{i=1}^{N} \vec{r}_i \times \left(\frac{-A_i}{2\pi} \bar{I}^2_{0,i} \cdot \hat{n}_i + a_{2,i} \frac{-A_i}{2\pi} \hat{n}_i \hat{n}_i \cdot \bar{I}^1_{0,i} + \rho_i s_i \frac{-A_i}{2\pi} (2\hat{n}_i \hat{n}_i - U) \cdot \bar{I}^2_{0,i} \cdot \hat{n}_i \right) \tag{2}$$

$$\bar{\vec{C}}_1 = \sum_{i=1}^{N} \vec{r}_i \times \left(\frac{-A_i}{\pi} \bar{I}^2_{c,i} \cdot \hat{n}_i + a_{2,i} \frac{-A_i}{\pi} \hat{n}_i \hat{n}_i \cdot \bar{I}^1_{c,i} + \rho_i s_i \frac{-A_i}{\pi} (2\hat{n}_i \hat{n}_i - U) \cdot \bar{I}^2_{c,i} \cdot \hat{n}_i \right) \tag{3}$$

$$\bar{\vec{D}}_1 = \sum_{i=1}^{N} \vec{r}_i \times \left(\frac{-A_i}{\pi} \bar{I}^2_{s,i} \cdot \hat{n}_i + a_{2,i} \frac{-A_i}{\pi} \hat{n}_i \hat{n}_i \cdot \bar{I}^1_{s,i} + \rho_i s_i \frac{-A_i}{\pi} (2\hat{n}_i \hat{n}_i - U) \cdot \bar{I}^2_{s,i} \cdot \hat{n}_i \right) \tag{4}$$

As can be seen, the coefficients are directly correlated to the optical, thermal, and geometrical properties of each facet. The simplest satellite model that can be used (which will be described in Section 3.1) will be composed of two facets where the following relationships hold true.

$$\begin{aligned}
\vec{r}_1 &= \vec{r}_2 \\
\hat{n}_1 &= -\hat{n}_2 \\
\hat{n}_1\hat{n}_1 &= \hat{n}_2\hat{n}_2 \\
A_1 &= A_2 \\
\bar{I}^1_{0,1} &= -\bar{I}^1_{0,2} \\
\bar{I}^2_{0,1} &= \bar{I}^2_{0,2}
\end{aligned}$$

Using these relationships and the fact that there are only two facets, the averaged coefficients can be simplified as shown in Eqs. 5, 6 and 7, where $\Delta a_2 = a_{2,1} - a_{2,2}$ and $\Delta\rho s = \rho s_1 - \rho s_2$.

$$\vec{\bar{C}}_0 = \vec{r}_1 \times \left[\left(\frac{-A_1}{2\pi} \Delta a_2 \hat{n}_1 \hat{n}_1 \cdot \bar{I}^1_{0,1} \right) + \left(\frac{-A_1}{2\pi} \Delta \rho s (2\hat{n}_1 \hat{n}_1 - U) \cdot \bar{I}^2_{0,1} \right) \right] \tag{5}$$

$$\vec{\bar{C}}_1 = \vec{r}_1 \times \left[\left(\frac{-A_1}{\pi} \Delta a_2 \hat{n}_1 \hat{n}_1 \cdot \bar{I}^1_{c,1} \right) + \left(\frac{-A_1}{\pi} \Delta \rho s (2\hat{n}_1 \hat{n}_1 - U) \cdot \bar{I}^2_{c,1} \right) \right] \tag{6}$$

$$\vec{\bar{D}}_1 = \vec{r}_1 \times \left[\left(\frac{-A_1}{\pi} \Delta a_2 \hat{n}_1 \hat{n}_1 \cdot \bar{I}^1_{s,1} \right) + \left(\frac{-A_1}{\pi} \Delta \rho s (2\hat{n}_1 \hat{n}_1 - U) \cdot \bar{I}^2_{s,1} \right) \right] \tag{7}$$

2.2. Orbit Averaged Rotational Dynamics

Using the previously stated assumptions and moments we can find the average evolution of the angular velocity and obliquity of a satellite under YORP moments throughout a year. The derivation of these averaged equations of motion can be found in reference 5. The evolution of the angular velocity and obliquity averaged over one orbital period around the Sun, is given by Eq. 8 and by Eq. 9, respectively. Note that in Eq. 9, thermal lag is ignored.

$$\dot{\bar{\omega}}_z = \frac{G_1}{I_z a^2 \sqrt{1-e^2}} \bar{C}_{0,z} \tag{8}$$

$$\dot{\bar{i}}_s = \frac{G_1}{2\omega_z I_z a^2 \sqrt{1-e^2}} \left(\bar{C}_{1,x} + \bar{D}_{1,y} \right) \tag{9}$$

We can see from these equations that the evolution of the angular velocity of a satellite will only be dependent on the z-component of the averaged C_0 coefficient, while the obliquity is solely dependent on the x-component of the averaged C_1 coefficient and y-component of the averaged D_1 coefficient. It is important to point out however, that the dynamics of angular velocity and solar inclination are coupled together. The Fourier coefficients will vary as the inclination evolves, therefore, the rate of change of angular velocity is indirectly dependent on the evolution of the obliquity.

3. SENSITIVITY ANALYSIS

To determine the sensitivity of the YORP coefficients to the optical, thermal and geometrical parameters of a satellite a simple model is used to represent an inactive satellite. The optical, thermal and geometrical properties of this model are then varied to account for all possible values and the YORP coefficients are found. The YORP coefficients for the different cases are analyzed to determine how they change as the parameters are altered. In addition the coefficients are used to determine possible long term behaviors for inactive satellites in GEO. The following sections give a description of the model used in this work and the results obtained.

3.1. Model Description

The model used for this sensitivity analysis is the most simple satellite model that can be used to represent some satellites in GEO. The model is composed of a symmetric bus with one symmetric appendage. Many satellites that use the Boeing 376 bus will have this same configuration where the appendage is an antenna. The satellite model and coordinate frame used for this study is shown in Figure 1.

For this analysis we are concerned with the effects of optical and thermal properties on the averaged coefficients. Therefore, the CM is located at the center of the bus (i.e. the mass of the appendage is ignored). The geometrical effects are considered by rotating the appendage about the y-axis. In addition, since the bus of the satellite is symmetric we only consider the averaged coefficients describing the torques acting on the appendage of the satellite. As previously mentioned, the model is composed of two facets, one for the front and one for the back of the appendage.

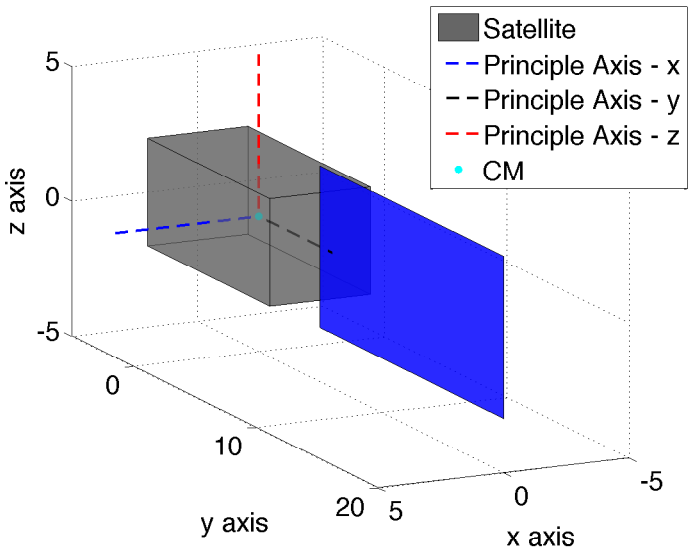

Figure 1: Satellite Model

3.2. Results

To analyze the possible long term behavior of the angular velocity and obliquity for this simple satellite model, we look at all possible $\Delta\rho s$ and Δa_2 values and determine its effects on the average coefficients. Furthermore, the appendage is rotated about the y-axis so that the normal vector varies as well. The possible values for ρ, s, ϵ_f and ϵ_b ranges from 0 to 1. Recall that $a_{2,i}$ has a combination of all of these values, so we must first find the possible combinations for $\Delta\rho s$ and Δa_2, these are shown in Figure 2.

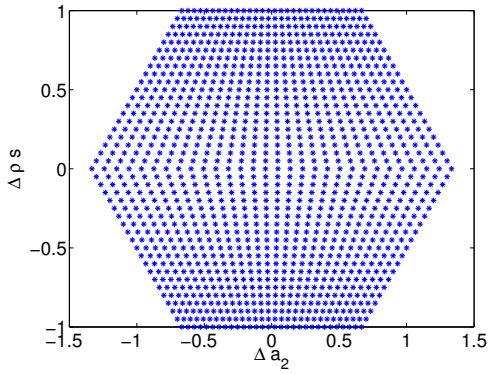

Figure 2: Possible Values for $\Delta\rho s$ and Δa_2

Note that as $\Delta\rho s$ varies the possible values of Δa_2 changes. We vary $\Delta\rho s$ by increments of 0.1 and Δa_2 in a way such that 10 values are always tested starting and ending with the limits of possible values. The satellite's appendage was rotated about the y-axis in increments of 10^o. However, for the results of this work we have selected only a few cases that show the general effects of varying all of these parameters.

Recall, the evolution of the angular velocity will be solely affected by $\bar{C}_{0,z}$. Figures 3a - 3d show the averaged $C_{0,z}$ coefficient over obliquity, as $\Delta\rho s$ and Δa_2 change for a satellite model where the appendage is rotated 30^o about the y-axis.

From Figure 3 we can see how varying $\Delta\rho s$ and Δa_2 affects the averaged $C_{0,z}$ coefficient which will directly impact the evolution of the angular velocity. We note that as Δa_2 changes the magnitude of the z component of the averaged C_0 coefficient changes, however, the general shape of the curve (as a function of obliquity) remains the same.

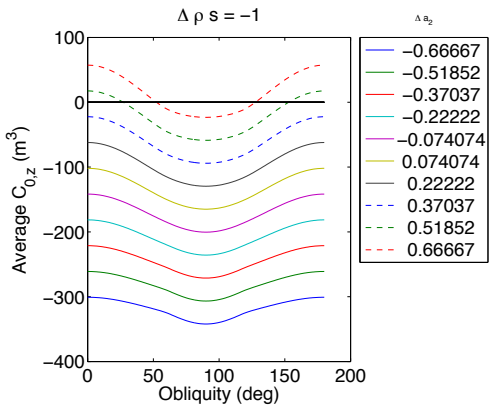

(a) Averaged $C_{0,z}$ Coefficients for 30^o appendage rotation - $\Delta\rho s = -1$

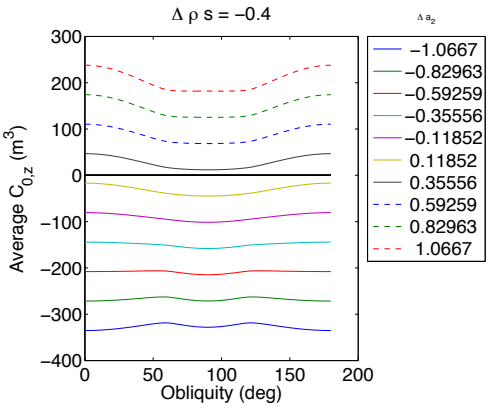

(b) Averaged $C_{0,z}$ Coefficients for 30^o appendage rotation - $\Delta\rho s = -0.4$

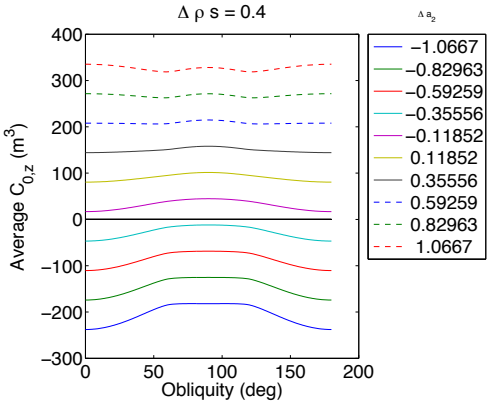

(c) Averaged $C_{0,z}$ Coefficients for 30^o appendage rotation - $\Delta\rho s = 0.4$

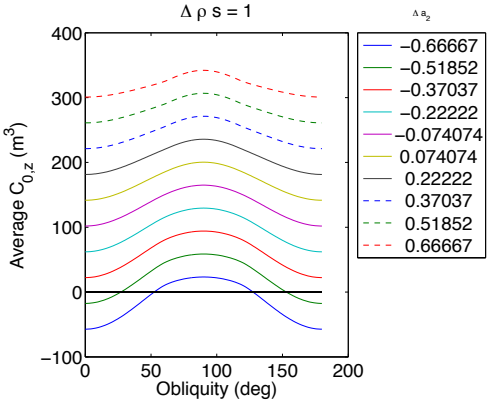

(d) Averaged $C_{0,z}$ Coefficients for 30^o appendage rotation - $\Delta\rho s = 1$

Figure 3: Averaged $C_{0,z}$ Coefficients for 30^o appendage rotation

It can be seen that regardless of the value of $\Delta\rho s$, the smaller Δa_2 the smaller that the averaged $C_{0,z}$ coefficient is. Figure 3 also shows that as $\Delta\rho s$ increases in value, the magnitude of the coefficient increases as well. Furthermore, we see that negative values of $\Delta\rho s$ result in coefficient curves that are inverses of those that resulted positive values of $\Delta\rho s$.

Note that an all positive coefficient would indicate a continuously increasing angular velocity, an all negative coefficient a continuously decreasing angular velocity and a coefficient which crosses zero will change spin direction at the obliquity value for the zero crossing. From Figure 3 we see that all three behaviors are possible. Varying $\Delta\rho s$ will change which of these behaviors occurs for a given curve at a given Δa_2 value.

Figures 4a - 4d show the averaged $C_{0,z}$ coefficient over obliquity, as $\Delta\rho s$ and Δa_2 change for a satellite model where the appendage is rotated 60^o about the y-axis.

From Figure 4 we can see how varying $\Delta\rho s$ and Δa_2 affects the averaged $C_{0,z}$ coefficient, which will directly impact the evolution of the angular velocity. Again, as Δa_2 changes the magnitude of the z component of the averaged C_0 coefficient changes, however, the general shape of the curve (as a function of obliquity) remains the same. As with the 30^o rotation, regardless of the value of $\Delta\rho s$, the smaller Δa_2 the smaller that the averaged $C_{0,z}$ coefficient is. Figure 4 also shows that as $\Delta\rho s$ increases in value, the magnitude of the coefficient increases as well. Furthermore, we see that negative values of $\Delta\rho s$ result in coefficient curves that are inverses of those that resulted positive values of $\Delta\rho s$. From Figure 4 we see that once again all three possible long term behaviors can occur. Varying $\Delta\rho s$ will change which of these behaviors occurs for a given curve at a given Δa_2 value.

While we note that varying $\Delta\rho s$ and Δa_2 has the same effects on the averaged $C_{0,z}$ coefficient regardless of the

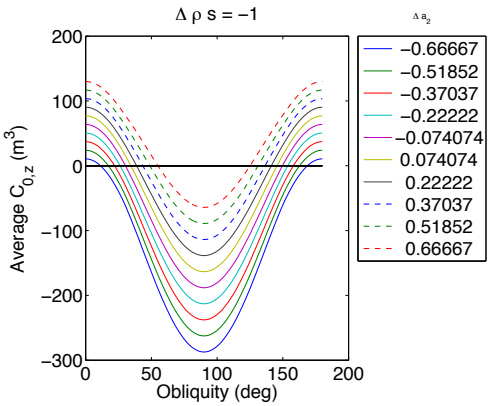

(a) Averaged $C_{0,z}$ Coefficients for 60^o appendage rotation - $\Delta\rho s = -1$

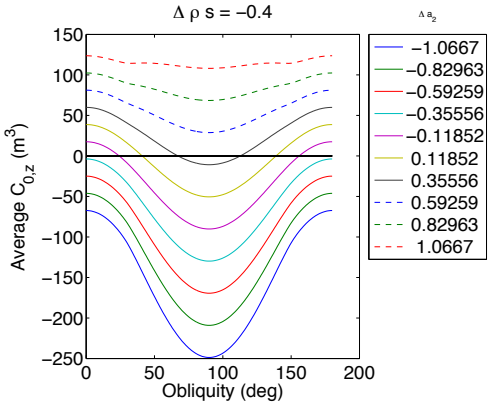

(b) Averaged $C_{0,z}$ Coefficients for 60^o appendage rotation - $\Delta\rho s = -0.4$

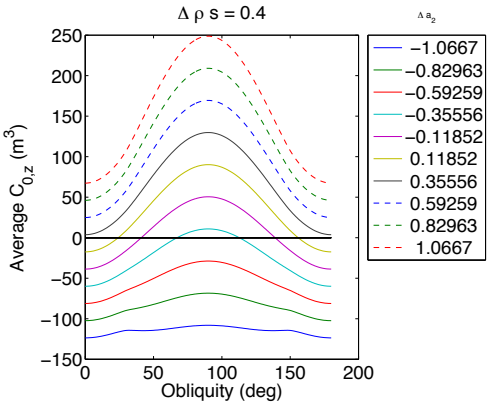

(c) Averaged $C_{0,z}$ Coefficients for 60^o appendage rotation - $\Delta\rho s = 0.4$

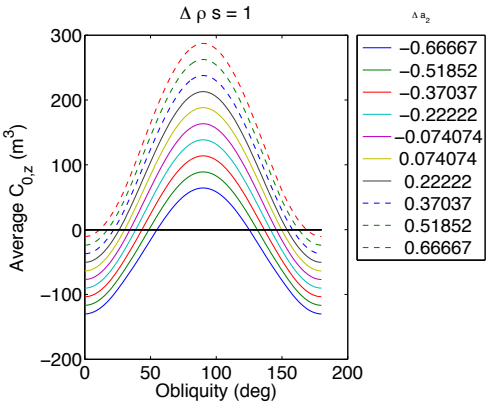

(d) Averaged $C_{0,z}$ Coefficients for 60^o appendage rotation - $\Delta\rho s = 1$

Figure 4: Averaged $C_{0,z}$ Coefficients for 60^o appendage rotation

angle of the appendage, changing the angle has an effect as well. A higher angle of rotation leads to more tightly packed averaged $C_{0,z}$ curves as Δa_2 varies. In addition, the curves are more sinusoidal when a higher angle of rotation is used for the appendage. This results in a change in the long term behavior of the satellite. For example, when $\Delta\rho s = 1$ and the appendage is rotated at 60^o, all curves (regardless of Δa_2 value) will have a zero crossing, indicating a change in spin direction of the satellite. However, only a few curves exhibit this behavior when when $\Delta\rho s = 1$ and the appendage is rotated at 30^o.

Now recall that the evolution of the obliquity will depend only on $\bar{C}_{1,x} + \bar{D}_{1,y}$. Figures 5a - 5d show $\bar{C}_{1,x} + \bar{D}_{1,y}$ over obliquity, as $\Delta\rho s$ and Δa_2 change for a satellite model where the appendage is rotated 30^o about the y-axis.

From Figure 5 we can see how varying $\Delta\rho s$ and Δa_2 affects $\bar{C}_{1,x} + \bar{D}_{1,y}$, which will directly impact the evolution of the obliquity. We note that as Δa_2 varies the magnitude of the sum of the coefficients changes and as the magnitude increases and goes from negative to positive, the curve is inverted. Unlike the $\bar{C}_{0,z}$ coefficient, as Δa_2 increases $\bar{C}_{1,x} + \bar{D}_{1,y}$ decreases in magnitude. We also note that in this case, the curves that result from negative values of $\Delta\rho s$ are not inverse of those that result from positive $\Delta\rho s$ values, but rather are the exact same curves.

It can be seen that all curves, regardless of $\Delta\rho s$ or Δa_2 values, are zero when the obliquity is zero, 90 or 180^o. In general, if the curve is positive the obliquity will increase and it will decrease if the curve is negative. We note that for the curves that are positive between 0 and 90^o of obliquity and crosses zero at 90^o the obliquity will eventually approach and remain at 90^o. Furthermore, if a curve is negative between 0 and 90^o the obliquity will approach and remain at 0^o. From Figure 5 we can see that both scenarios occur and the dominating factor in this case is Δa_2.

Figures 6a - 6d show $\bar{C}_{1,x} + \bar{D}_{1,y}$ over obliquity, as $\Delta\rho s$ and Δa_2 change for a satellite model where the appendage

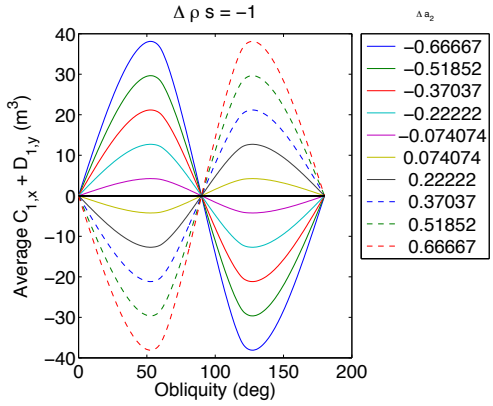

(a) Averaged $C_{0,z}$ Coefficients for 30^o appendage rotation - $\Delta\rho s = -1$

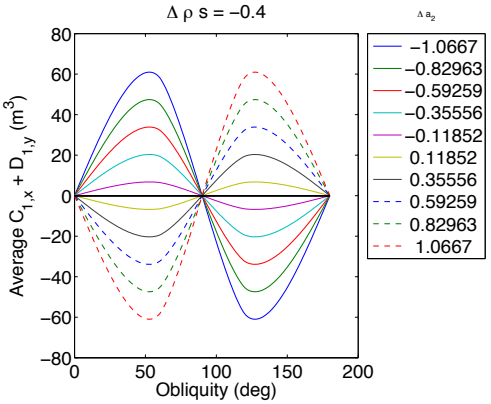

(b) $\bar{C}_{1,x} + \bar{D}_{1,y}$ for 30^o appendage rotation - $\Delta\rho s = -0.4$

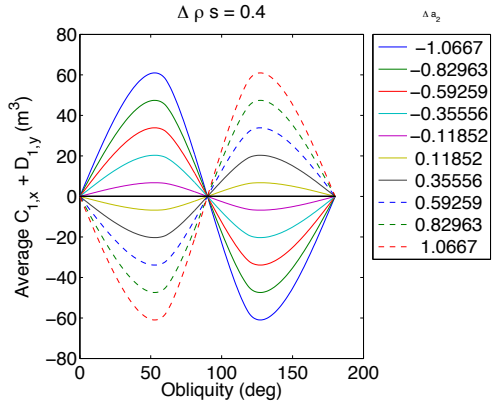

(c) $\bar{C}_{1,x} + \bar{D}_{1,y}$ for 30^o appendage rotation - $\Delta\rho s = 0.4$

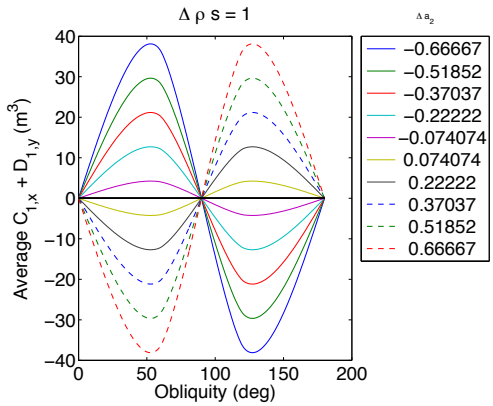

(d) $\bar{C}_{1,x} + \bar{D}_{1,y}$ for 30^o appendage rotation - $\Delta\rho s = 1$

Figure 5: $\bar{C}_{1,x} + \bar{D}_{1,y}$ for 30^o appendage rotation

is rotated 60^o about the y-axis.

From Figure 6 we can see how varying $\Delta\rho s$ and Δa_2 affects $\bar{C}_{1,x} + \bar{D}_{1,y}$ which will directly impact the evolution of the obliquity. We note that as Δa_2 varies the magnitude of the sum of the coefficients changes. As the magnitude of Δa_2 increases, the magnitude of sum of the coefficients decreases. We also note that in this case, the curves that result from negative values of $\Delta\rho s$ are inverse of those that result from positive $\Delta\rho s$ values.

It can be seen from these figures that as $\Delta\rho s$ changes the curves change in such a way that there is an additional zero crossing. The additional zero crossing that occurs when $\Delta\rho s = -0.4$ will not change the long term behavior for the satellite with the curve that has this crossing since the curve is negative between 0^o of obliquity and the obliquity at which the zero crossing occurs. However, the additional zero point when $\Delta\rho s = 0.4$ will change the behavior since the curve is positive between 0^o of obliquity and the obliquity at which the zero crossing occurs. In this case, the obliquity will approach and remain at the obliquity at which this zero crossing occurs. Note that these additional zero points occur as the angle of rotation for the appendage increases.

The averaged YORP coefficients that directly impact the evolution of angular velocity and obliquity are extremely sensitive to variations in the optical, thermal and geometrical parameters of the facets making up a satellite. As was shown here varying these parameters can drastically change the long term behavior of a satellite. While some parameter combinations will lead to simple behavior changing one parameter slightly can result in more complex dynamics, for example adding a stable equilibrium for the evolution of the obliquity. This shows the importance of having good knowledge of materials making up satellites and how they degrade over time in the space environment in order to accurately model dynamics and make long term predictions.

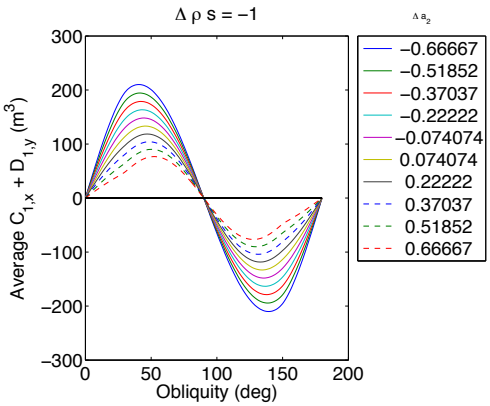

(a) Averaged $C_{0,z}$ Coefficients for 60^o appendage rotation - $\Delta\rho s = -1$

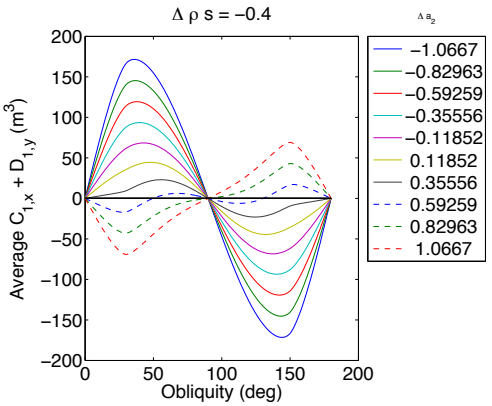

(b) $\bar{C}_{1,x} + \bar{D}_{1,y}$ for 60^o appendage rotation - $\Delta\rho s = -0.4$

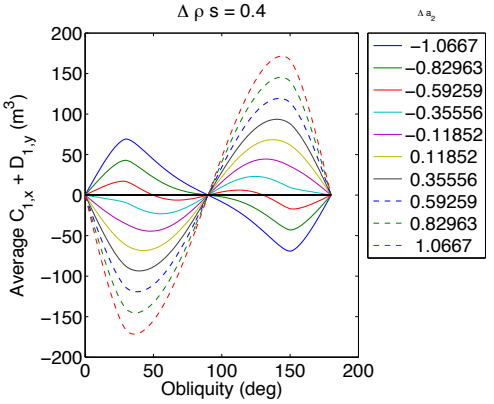

(c) $\bar{C}_{1,x} + \bar{D}_{1,y}$ for 60^o appendage rotation - $\Delta\rho s = 0.4$

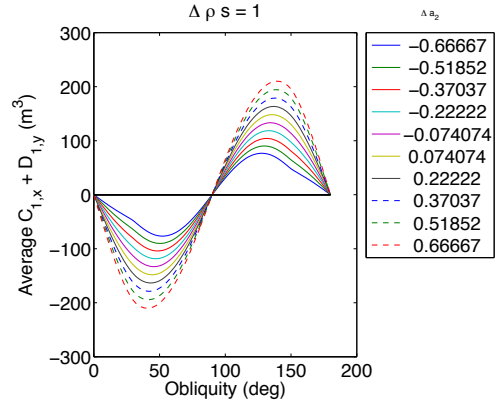

(d) $\bar{C}_{1,x} + \bar{D}_{1,y}$ for 60^o appendage rotation - $\Delta\rho s = 1$

Figure 6: $\bar{C}_{1,x} + \bar{D}_{1,y}$ for 60^o appendage rotation

4. CONCLUSION

Observations of inactive satellites in GEO have demonstrated that the rotational periods of these objects are changing over time. Furthermore, the evolution of the rotational periods can vary from satellite to satellite. The YORP effect, which has been well studied and documented for asteroids, has been recently offered as a possible explanation for the observed changes in rotational periods of inactive satellites. The YORP effect however, is highly dependent on the optical, thermal and geometrical parameters of the satellite. This work analyzed the sensitivity of the moments created by the YORP effect on a satellite to variations in these three parameters. The results showed that small changes in these can lead to very different long term behavior of the satellite. If materials degrade in different manners in the space environment for various satellites this could offer an explanation as to why the rotational periods of inactive satellites evolve differently over time. This work further motivates the importance of understanding the properties of materials making up satellites and how those might change after being in space for a period of time.

5. ACKNOWLEDGMENT

This research was supported by the NSF Graduate Research Fellowship Program and the FAA Center of Excellence for Commercial Space Transportation Research. The authors acknowledge support through Air Force Office of Scientific Research grant FA9550-11-1-0188.

References

[1] Papushev, P., Karavaev, Y., & Mishina, M., Investigations of the evolution of optical characteristics and dynamics of proper rotation of uncontrolled geostationary artificial satellites, Advances in Space Research, 416-1422, 2009.

[2] Karavaev, Y., Kopyatkevich, R.M., Mishina, M.N., Mishin, G.S., Papushev, P.G., & Shaburov, P.N., The Dynamic Porperties of Rotation and Optical Characteristics of Space Debris at Geostationary Orbit, Advances in the Astronautical Sciences, 1457-1466, 2004.

[3] Taylor, P.A., Margot, J.L., Vokrouhlicky, D., Scheeres, D.J., Pravec, P., Lowry, S.C., Fitzsimmons, A., Nolan, M.C., Ostro, S.J., Benner, L.A., Giorgini, J.D., & Magr, C., Spin rate of asteroid (54509) 2000 PH5 increasing due to the YORP effect, Science, 274-27 , 2007.

[4] Rubincam, D., Radiative Spin-up and Spin-down of Small Asteroids, Icarus, 2-11, 2000.

[5] Scheeres, D.J., The dynamical evolution of uniformly rotating asteroids subject to YORP, ICARUS, 430-450,2007.

[6] Albuja, A.A. and Scheeres, D.J., Defunct Satellites, Rotation Rates and the YORP Effect, Proceedings of the Advanced Maui Optical and Space Surveillance Technologies Conference [CD], Wailea, Hawaii, 156-163, 2013